J. Phys. B: At. Mol. Opt. Phys. **42** (2009) 065204 (10pp) doi:10.1088/0953-4075/42/6/065204

Elastic electron scattering from hydrogen molecules at high-momentum transfer

M Vos and M R Went

Atomic and Molecular Physics Laboratories, Research School of Physics and Engineering,
The Australian National University, Canberra 0200, Australia

E-mail: maarten.vos@anu.edu.au

Received 22 December 2008, in final form 12 February 2009
Published 9 March 2009
Online at stacks.iop.org/JPhysB/42/065204

Abstract

In high-momentum transfer electron scattering experiments the 'elastic signal' is separated into different components, depending on the mass of the scatterer due to the recoil effect. Here, we compare the peak positions and shapes obtained from H_2, D_2 and HD with theory developed for neutron scattering experiments at similar momentum transfer. The hydrogen peak width increases with increasing momentum transfer. The observed width is in line with the vibrational properties of H_2. The line shape of the elastic peak is also studied for HD and D_2 molecules. The H peak of HD is broader than the H peak of H_2, and the D peak of D_2 is broader than the D peak of HD. We also investigate elastic scattering at high-momentum transfer of gas mixtures containing hydrogen and either heavy (Xe) or light (He) noble gases. Changing the energy of the incoming beam changes for the Xe/H_2 gas mixture the ratio of the Xe to H_2 signal in a dramatic way, but for the He/H_2 mixture the intensity ratio is constant. The energy dependence of the observed intensity ratio is in both cases accurately described by 'standard' differential elastic cross section calculations. Results are discussed in the context of a recent report of anomalies in electron scattering results of H_2 under similar experimental conditions and anomalous neutron scattering results of H_2, D_2 mixtures and HD. An in-depth look at the peak shape of hydrogen reveals deviations from a simple Gaussian line shape which are interpreted to be, at least in part, a consequence of the bonding of the nucleus to a molecule.

(Some figures in this article are in colour only in the electronic version)

1. Introduction

In a large-angle scattering experiment, an incoming electron (energy E_0, momentum $\boldsymbol{k}_0$) scatters from a target. Electrons with momentum $\boldsymbol{k}_1$ and energy E_1 are detected by an analyser. The directions of $\boldsymbol{k}_0$ and $\boldsymbol{k}_1$ are determined by the positioning of the electron gun and analyser. There is thus a momentum transfer in the collision $\boldsymbol{q} = \boldsymbol{k}_0 - \boldsymbol{k}_1$. When scattering from a stationary atom, it will start moving and hence acquire kinetic energy in the particle–atom collision. The energy of the scattered particle is reduced by the (mean) recoil energy, $\overline{E_\mathrm{r}} = q^2/2m_\mathrm{a}$, with m_a being the mass of the atom. It is thus possible to determine the mass of the scattering atom using high-energy electrons (>1 keV) scattered over large angles (>90°) [1, 2]. If the scattering atom had a momentum $\boldsymbol{p}$ before the collision, then the recoil energy E_r is given by the difference in the kinetic energy of the scattering atom before and after the collision:

$$E_\mathrm{r} = \frac{(\boldsymbol{p}+\boldsymbol{q})^2}{2m_\mathrm{a}} - \frac{p^2}{2m_\mathrm{a}} = \frac{q^2}{2m_\mathrm{a}} + \frac{\boldsymbol{p}\cdot\boldsymbol{q}}{m_\mathrm{a}}. \quad (1)$$

The first observation of recoil shifts of the elastic peak in the field of electron scattering was made by Boersch *et al* [3], using keV electrons deflected from carbon films. More recently, these experiments were extended to a gas phase [4]. The peak is centred on the mean recoil energy $\overline{E_\mathrm{r}} = q^2/2m_\mathrm{a}$ but its shape contains the Doppler profile of the velocity distribution of the scattering atoms. Investigation of the peak shape thus reveals the probability that the scatterer has a momentum component along $\boldsymbol{q}$.

For free atoms (noble gases), the momentum distribution is that of a classical gas. For each of the momentum components (p_x, p_y, p_z), the momentum distribution is such that $\int p_c^2/2m_\mathrm{a} = 1/2kT$. For an atom bound to a molecule (or

a solid) the momentum distribution is *not* that of a classical gas, as it is affected by the rotational and vibrational properties of a molecule. For H_2, the vibrational energy is 0.55 eV (0.39 eV for D_2 and 0.47 eV for HD) [5]. Thus at ambient temperature, and below, only the vibrational ground state is occupied. The energy of this state is $1/2\hbar\omega$, equally divided into kinetic and potential energies. For H_2 and D_2, the kinetic energy is equally divided over both atoms. Thus the kinetic energy of each atom, due to the vibrational mode, is $1/8\hbar\omega$ (0.068 eV for H in H_2 and 0.048 eV for D in D_2), considerably larger than $1/2kT$. As the centre of mass is not affected by the vibrational motion, the H and D atoms in HD will have the same magnitude of momentum (but opposite sign). This means that the vibrational kinetic energy ($p^2/2m_a$) is divided over H and D as 2:1.

For the two rotational modes the spacing of the rotational levels is such that more than one rotational level has significant occupation at room temperature, and we assume on average $1/2kT$ energy for each rotational mode. The same is true for the three translational degrees of freedom. The kinetic energy of the translational and rotational levels is shared equally (for H_2 and D_2) over both nuclei, so the contribution to the kinetic energy for each nucleus of these 5 degrees of freedom is $5/4kT$ (0.031 eV at room temperature). Thus, at room temperature, the contribution of the vibrational mode to the peak width is larger than the contributions of all other degrees of freedom combined.

If all degrees of freedom have a Gaussian-shaped momentum distribution, then the Doppler width σ_{Dop} of the elastic peak and the mean total kinetic energy $\langle E_{\mathrm{kin}}\rangle$ are related by [6, 7]

$$\sigma_{\mathrm{Dop}} = \sqrt{(4/3)\langle E_{\mathrm{kin}}\rangle \overline{E_{\mathrm{r}}}}. \tag{2}$$

From neutron measurements, taken at cryogenic temperatures, it is clear that for para-hydrogen the momentum density distributions decrease slower with increasing magnitude than predicted by a simple Gaussian line shape [8]. This is understood theoretically based on the spherical symmetry of the nuclear wavefunction of para-hydrogen in its ground state. In our experiment, nominally at room temperature and containing ortho- and para-hydrogen, several rotational states have non-zero occupancy. This could possibly affect the observed line shape. Thus, we investigate if the line shape can indeed be fully described by a Gaussian.

The picture sketched here is very simple. It assumes that the electron scatters from a single atom and not from a molecule (for scattering from molecules in the gas phase) or even from a crystal (scattering from a solid). This is called the incoherent approximation, and it is applicable in the limit of high-momentum transfer. Another assumption made here is that the energy of the scattering atom can be described by $q^2/2m_a$, that is, it acts as a free particle. This assumption is referred to as the impulse approximation. It is exact only for $q \to \infty$. These theories were developed and tested for neutron scattering [8–11]. Here, the prototypical test case was neutron scattering from hydrogen molecules. At intermediate momentum transfer, different peak shapes were observed. These observations were attributed to a failure of impulse approximation.

It has become clear that a similar range of momentum transfer can be accessed by electron scattering and that the energy resolution is nowadays good enough to resolve the recoil energy. These electron scattering experiments were first done on solids, such as polymers [1] and graphite [12], and later on gases as well, in particular CH_4 [4]. This paper describes the first survey of electron scattering results from hydrogen atoms for $|q|$ values between 15 and 39 atomic units (au).

In a recent letter, Cooper *et al* reported a gas-phase electron Compton scattering (ECS) study of electrons scattering from a 50% H_2, 50% D_2 mixture and from pure HD molecules [13]. The intensity of the proton peak was equal to the intensity of the deuteron peak, when scattering from HD, but for the H_2/D_2 mixture the proton peak area was smaller than the deuteron one. These experiments were tentatively explained as a consequence of the influence of quantum entanglement on the H_2 cross section, an explanation that is also invoked to describe anomalous scattering intensities in neutron Compton scattering (NCS) experiments (see, for example, [14–16]). Liquid, 50% H_2, 50% D_2 mixtures and liquid HD were also studied by NCS [17]. These experiments had a comparable momentum transfer (15–60 au) to the electron scattering experiment described here. In the neutron experiment, a deviation of the expected H intensity (relative to that of D) was found for the H_2/D_2 mixture and *also* for the HD sample [17]. In the neutron scattering experiment, the recoil energy was generally larger than the hydrogen dissociation energy (4.7 eV), whereas in the experiment of Cooper *et al* [13] the recoil energy was less than this value. This was suggested as the explanation in [13] why HD showed an anomalous peak ratio in the NCS experiment but not in the ECS experiment. In this paper, we will show data where $\overline{E_{\mathrm{r}}}$ is larger than the dissociation energy.

The interest in these studies is related to the scattering time. It is given by

$$\tau = 1/(q v_0), \tag{3}$$

with v_0 is the root-mean-square velocity of the atom [9, 10]. These scattering experiments (both neutron and electron) probe the system over an extremely short time (attoseconds), possibly shorter than the presumed decoherence time of a hydrogen atom with its environment. This opens the possibility that quantum effects could influence the observed scattering intensity [18].

In the experiment of Cooper *et al*, the H and D contributions are only partly separated at the highest momentum transfer **q** obtainable in the McMaster apparatus (100° and 2250 eV, corresponding to $|q| = 19.7$ au). The electron scattering spectrometer at the Australian National University (ANU) is able to operate at a larger scattering angle (135°) and energies (up to 6 keV); hence, it can study collisions with $|q|$ up to 39 au [4]. The separation of the different elements (proportional to q^2) is such that in this spectrometer, the D and H elastic peaks can be separated completely. Thus, we can compare the elastic peak widths of H and D in HD and in H_2 and D_2 with theoretical expectations.

At the ANU, we can vary the energy of the incoming beam significantly while still separating the different scatterers. This

changes the scattering time τ (equation (3)), a quantity that plays a crucial role in the theory of attosecond entanglement. Changing the energy of the incoming electrons will not affect the composition of the scattering gas or the shape of the gas plume. Thus if anomalies are present *and* these anomalies are a function of the scattering time τ then, for mixtures, we should see variations in the relative intensity of the hydrogen peak with E_0. For heavy elements the calculations of the DCS for electrons, taking into account the effect of screening of the nucleus by the target electrons, show pronounced deviations from the Rutherford cross section. These deviations are particularly strong for Xe at a scattering angle of 135°. The same calculation shows that screening effects are very minor for He. Separation of the H and He elastic peaks is somewhat ($\simeq$25%) smaller than that of the H–Xe case, but still sufficient to separate both components. We studied H_2–Xe and H_2–He mixtures over a range of q values for signs that the collision time τ affects the H cross section.

2. Experimental details

The spectrometer is described in detail in [4], where it was used to study CH_4. Currently, the gun has a BaO cathode to reduce the thermal spread of the beam. A hemispherical analyser is used to detect electrons scattered over 135°. It operates at a pass energy of 200 eV. As the cross sections are very low for large-angle scattering (e.g. 5×10^{-23} cm^2 sr^{-1} for scattering from H at 135° at 6 keV), it is essential to have a two-dimensional detector measuring a range of angles and energies simultaneously. The energy resolution, as judged from the peak full width half-maximum (FWHM) of heavy targets like Xe, is 0.5 eV. Each scan consists of a signal and background run. During the signal run, the gas enters the chamber through a needle (1 cm long, 1 mm inner diameter, pointing downwards) just above the interaction region. During the background run the gas enters the chamber away from the interaction region, and electrons can be detected due to interaction with the residual atoms in the vacuum and possibly the halo of the beam hitting the gas needle. The actual result is the difference of the signal and the background run.

Unfortunately, the zero point of the spectrometer depends slightly on the lens settings. To fix the energy scale, and to be able to ascertain that the spectrometer has a good resolution, we often add a small amount of a reference gas, in practice either Xe or He. These atoms are not bonded and thus the recoil energy here is indeed $q^2/2m_a$. Using this value, the sharp peak of the reference gas allows for an accurate determination of the zero point of the energy scale.

Sometimes, it is not desirable to have a reference gas; for example, when one studies details of the peak shapes at q values where the reference gas and hydrogen are not completely separated. In that case a separate Xe measurement was done, with exactly the same spectrometer settings, just before or after the actual hydrogen run. This method is not as accurate as using a gas mixture, since the presence of hydrogen affects the performance of the BaO cathode. Emission current from the cathode increased threefold when the cathode was exposed to hydrogen, presumably as hydrogen

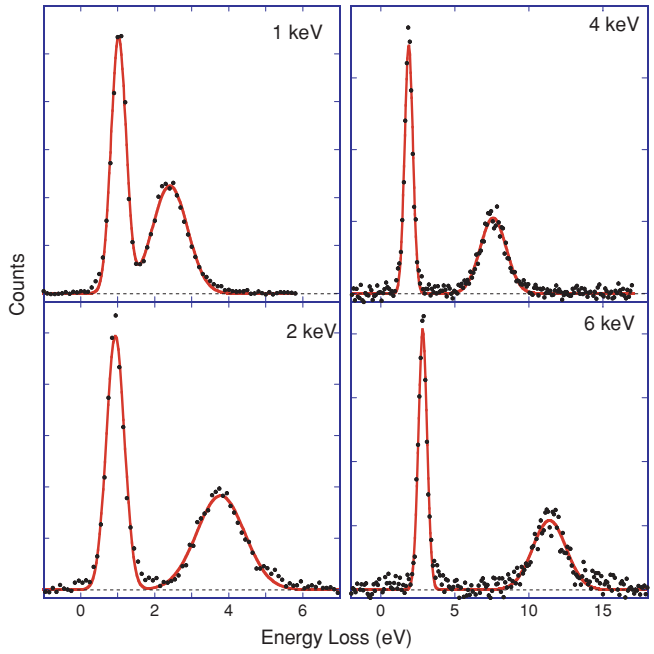

Figure 1. Spectra of a He–H_2 mixture for incoming energies E_0, as indicated.

affects the cathode work function. The effect of hydrogen was tested by adding a second leak valve to the chamber, through which H_2 was admitted, well away from the interaction region. Measuring the Xe elastic peak with H_2 in the background (partial H_2 pressure 1.5×10^{-6} Torr) resulted in a shift of 0.15 eV of the Xe peak to lower energies (higher energy loss) compared to the measurement without H_2 in the background. The hydrogen exposure also caused a minor increase (10%) in the width of the Xe elastic peak, presumably due to the increased energy spread of the electron beam.

The energy loss spectrum of Xe has a relatively isolated structure at 8.44 eV relative to the elastic peak [19]. This was used to check the energy scale of the spectrometer. It was found in our spectrometer to be 8.5 ± 0.1 eV. Finally, the high voltage reading of the electron gun was cross-checked by comparing it to a high-precision 1 kV supply. The agreement was better than 1%.

3. Experimental results

3.1. H_2–He mixture

Under the conditions described here, the DCSs of H and He are reasonably well described by the Rutherford cross section, which scales as Z^2. The DCS of He is thus $\simeq$4 times that of H (and double that of H_2). Moreover, the velocity of a H_2 molecule will be $\sqrt{2}$ times the velocity of a He molecule, and hence H_2 will spend less time in the interaction region, just below the needle. Thus, in order to get an approximately equal signal of H and He, we prepared a mixture with a H_2:He partial pressures ratio of $2\sqrt{2}$:1.

The results, presented in figure 1 and summarized in table 1, indeed show two peaks in all spectra: a narrow one at low energy loss and one at $\approx$4$\times$ larger energy loss. The larger energy loss corresponds to scattering

from a single proton ($m_a = 1$), in spite of the fact that the proton is part of H_2. Both peaks are fitted with a single Gaussian. The separation of the two peaks (see table 3) is indeed given by $q^2/2m_H - q^2/2m_{He}$ and the agreement between the calculated and measured separation is good. The width of the He peak is close to the experimental resolution of the spectrometer, as obtained from Xe measurements: 0.5–0.6 eV FWHM ($\sigma = 0.2$–0.25 eV). This is somewhat surprising. If we assume a mean kinetic energy of the He atoms to be $3/2kT$ then one obtains, using equation (2), for $E_0 = 6$ keV a width (σ) at an ambient temperature of 0.37 eV. Corrected for the experimental resolution the observed width is at most 0.2 eV, just half the calculated value. Thus, the He momentum distribution is not the equilibrium distribution at room temperature.

Note that we are sensitive to the momentum component directed along the momentum transfer direction. In our spectrometer, the gas jet points downward and the momentum transfer direction is in the horizontal plane. There are two possible explanations for the He peak being sharper than expected.

- Due to the collimation in the beam, the velocity distribution has changed. As a consequence of the interaction of the atoms with the walls of the needle, the mean horizontal momentum component of the atoms emerging at the end of the needle is strongly reduced (at least by a factor of 2).
- There is cooling of the beam due to adiabatic expansion. For this mechanism, one needs collisions between the gas atoms to dominate over interactions of the atoms with the wall of the needle. It is a well-known and effective cooling mechanism, but it is usually associated with much higher driving pressures (hence more collisions between the gas molecules) than in our experiment, where we run typically at 2×10^{-6} torr using a turbo pump of 500 l s^{-1}.

If we take the He peak width as a measure of the experimental resolution, then one can extract the intrinsic H peak width from the measured H peak width. These values are shown in table 3 as 'σ H corr.'. With increasing E_0, the intrinsic width becomes larger. A fourfold increase of E_0 (from 1 to 4 keV) causes a doubling of the width (σ increases from 0.43 to 0.82 eV), in agreement with equation (1).

The ratio of the H to He peak area is close to 1:1 (see table 3), as expected for this gas mixture. These data could be taken to mean that the anomalous low cross section of H in H_2, reported in [13], is absent in the present experiment. However, we stress here that the arguments on which the expectation of an equal area is built are rather flimsy. For example, the velocity distribution of H and He coming out of the needle could well deviate from that of a classical gas in thermal equilibrium. Indeed, the small width of the He peak points in this direction. We are on a safer ground assuming that the effective composition of the target gas is unknown, but that it does not change with E_0. Then the rather constant ratio of the H to He peak intensity means that a cross section anomaly, if present, is not a strong function of the momentum transfer, i.e. the scattering time (see equation (3)). Indeed, this was also the conclusion of neutron measurements of the anomalous cross section of H in H_2 [17].

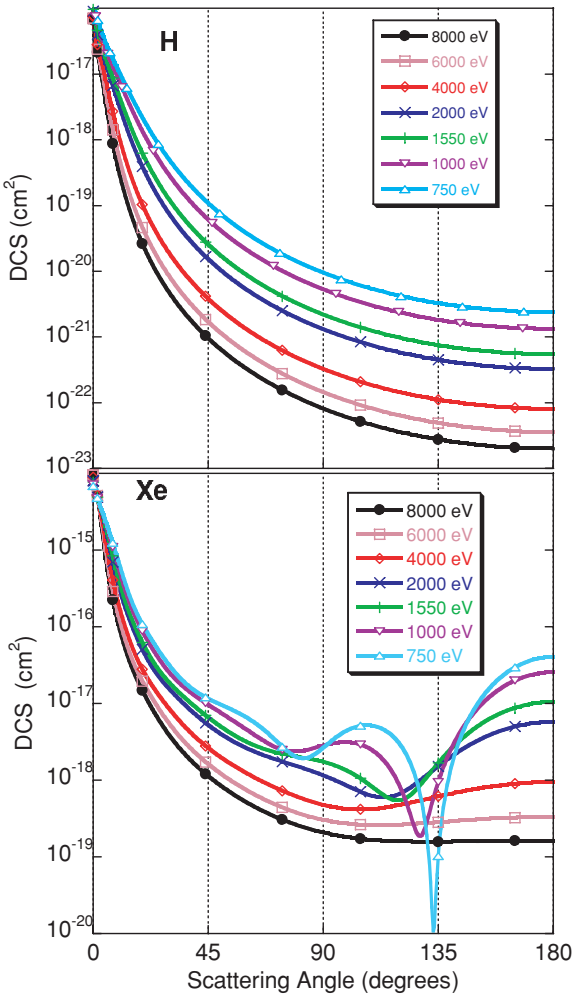

Figure 2. The DCS as calculated using ELSEPA for H and Xe, at the energies as indicated.

3.2. H_2–Xe mixture

If we use a heavy atom as Xe as a reference gas, then the separation of the two elastic peaks is slightly better than for H_2 and He. Moreover, the Doppler broadening of Xe is negligibly small. However, the Xe screening of the nuclear charge plays an important role and the DCS cannot be described by the Rutherford cross section. As a consequence, the ratio of the intensity of the Xe to H elastic peak becomes strongly dependent on E_0 (or the scattering angle). We used the ELSEPA package to calculate the DCS [20]. It includes the effect of screening, exchange and absorption, but polarization effects are negligibly small under these conditions and were not included. The results of these calculations are displayed in figure 2. For H, the cross section (except at small scattering angles) follows the Rutherford formula. For example, doubling the energy reduces the DCS by a factor of 4. For Xe, the picture is more complicated. For lower E_0 values, a very strong minimum develops close to 135°. This is where our analyser is positioned. As the cross sections are now so different, we made a mixture with a Xe:H_2 ratio of $\simeq$1:750. The result of the H_2, Xe mixture is shown in figure 3.

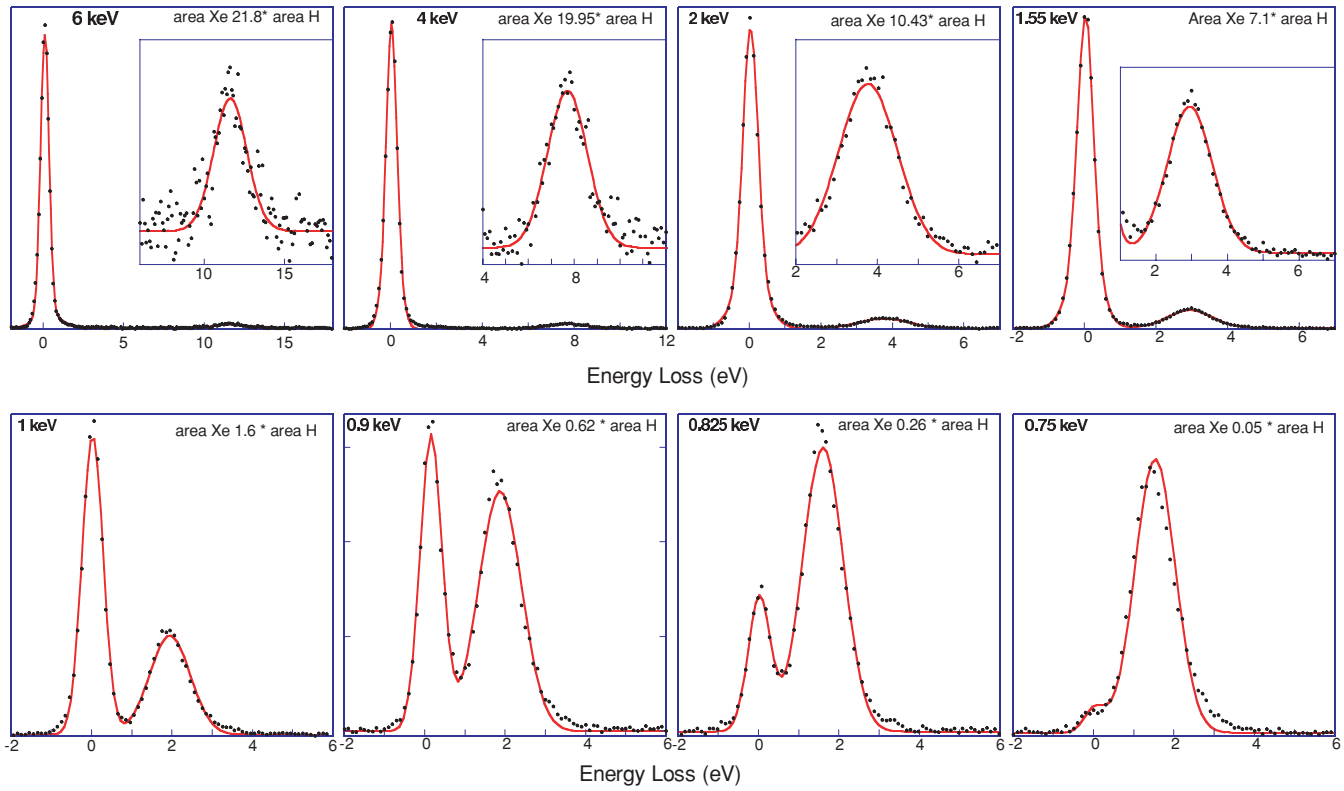

Figure 3. The spectra of a Xe–H_2 gas mixture as a function of E_0.

Table 1. Summary of the results for H_2, using He mixed with H_2 as a reference. The second and third columns contain the calculated and observed H–He peak separation, respectively. The corrected H peak width (σ H corr.) is calculated from the observed peak width (σ H total) assuming that the He peak width (σ He) is a measure of the experimental resolution. The last column shows the He–H peak intensity ratio.

E_0 (keV)	q (au)	ΔE calc (eV)	ΔE obs. (eV)	σ He (eV)	σ H total (eV)	σ H corr. (eV)	I_{He}:I_H
1.00	15.8	1.40	1.39	0.20	0.47	0.43	1:0.99
2.00	22.3	2.81	2.84	0.24	0.65	0.60	1:0.99
4.00	31.7	5.62	5.70	0.28	0.87	0.82	1:0.93
6.00	38.9	8.46	8.57	0.28	1.04	1.00	1:0.96

At high energy (e.g. 6 keV), the area of the hydrogen elastic peak is only 5% of that of Xe. Reducing E_0 down to 2 keV results in a doubling of the relative strength of the H signal. At even lower energies, the H signal dominates. At $E_0 = 750$ eV it is hard to extract the Xe contribution, as Xe is only a shoulder on the H peak. For each energy, the peak separation is again close to the values derived from equation (1).

In figure 4, we compare the observed intensity ratio with the scaled ratio of the calculated DCS of Xe and atomic H. The scaling factor used to get the best agreement was 280. There are 1500× more H atoms than Xe atoms in the mixture. However, the velocity distribution of H_2 and Xe will differ, and hence the time during which H and Xe linger in the interaction region is different. From the applied scaling factor (280) and H:Xe concentration ratio (1500:1), we conclude that Xe is $1500/280 = 5.3$ times longer in the interaction region than H_2. Based on the mass ratio, *and* assuming thermal equilibrium velocity distributions, the mean Xe velocity would be $\sqrt{m_{Xe}/m_{H_2}} = 8\times$ smaller than the mean H_2 velocity. This agreement is as good as can be expected for the rather basic mixing procedure followed.

If we assume that the H cross section is known (either given correctly by the Rutherford formula or calculations such as ELSEPA), then this experiment is a measurement of the DCS of Xe as a function of E_0 at a constant scattering angle. Traditionally, DCS measurements use a constant energy and change the scattering angle. Indeed data for Xe obtained in this mode exist at lower energies [21], and both measurement methods corroborate the theory. Here, we present these data to underline that screening is important in these elastic scattering experiments.

3.3. D_2 results

For D_2, the separation between a heavy reference gas and the D signal would be about half of that for H_2. Thus, peak separation would be more difficult. To avoid this problem, we measured pure Xe immediately before or after the measurement of D_2, without changing any of the voltages. The results are given in

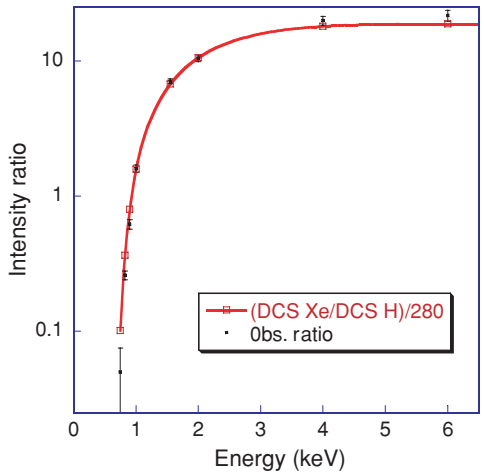

Figure 4. A comparison of the peak area ratio I_{Xe}/I_H as a function of the incoming energy E_0 with the calculated DCS ratio $(d\sigma/d\Omega_{Xe})/(d\sigma/d\Omega_H)$.

Table 2. Summary of the results for D_2, using a separate set of Xe measurements as a reference. Further as table 1.

E_0 (keV)	ΔE calc (eV)	ΔE obs. (eV)	σ Xe (eV)	σ D total (eV)	σ D corr. (eV)
1.00	0.92	0.91	0.26	0.36	0.27
2.00	1.84	2.04	0.24	0.48	0.41
4.00	3.68	3.94	0.27	0.59	0.52
6.00	5.54	5.85	0.29	0.70	0.61

table 2. Indeed, the separation of deuterons and Xe is smaller than that of protons and Xe. Also, the observed separation is not in as good an agreement with the calculated one as for the H_2–Xe case. This is, at least in part, due to the electron gun cathode work function lowering when exposed to hydrogen, resulting in a shift to higher energy of the emitted electrons. Indeed by subtracting 0.15 eV from the experimental separation (due to the change in the work function, as explained in section 2), the agreement becomes somewhat better. The width of the D peak is smaller than the width of the H peak at the same momentum transfer. Again, increasing E_0 by a factor of 4 results in a doubling of the peak width.

3.4. HD results

HD (97% pure) was purchased from Cambridge isotope laboratories. Unfortunately, after backfilling our measurement volume with this gas, there was some contamination with heavy impurities as is evident in the spectra shown in figure 5. From the separation of the H and D signals and the impurity signal, we conclude that the impurity signal is most likely due to a combination of C, N and O atoms. A 1% contamination with O_2 would give a signal that is $\simeq 1.28\times$ $(Z^2 \times 2/100)$ that of either H or D, as the cross section roughly scales with Z^2. The observed signal strength of the impurity is only $\simeq 0.2$ times that of H or D. For $E_0 = 2$ keV and above, the signal of this impurity was well separated from either the D or the H signal, so analysis in terms of H and D peak areas, peak separation and peak widths was not significantly affected by this impurity. It is of course possible that the impurity contains hydrogen as well (e.g. H_2O or CH_4), but the contribution of the impurity H component to the H signal would be very small, as even for the worst case (CH_4) the total H signal strength would be nine times less than the impurity (carbon) signal strength [4].

The interpretation of the measurement is thus not affected by the impurity. All three components were fitted with a single Gaussian, and the peak separation and peak width are reproduced in table 3. There is a good agreement between the calculated and measured H and D peak separation. The H and D peak widths are clearly different; after correction for experimental resolution, the H peak width is close to double the D peak width. From equation (1), it is clear that this implies that the momentum distribution of H atoms is approximately equal to the momentum distribution of D atoms. The contribution to the width of the (molecular) translational motion of the molecule would be equal for H and D, as the translational momentum of D is twice that of H. The observation that the width of H is twice the width of D is again an indication that translational motion has only a very minor impact on the observed peak width.

In this experiment, the peak area ratio of the H and D peaks approaches 1 with increasing energy. The fact that the H peak is slightly larger at lower E_0 values (2 and 4 keV) is probably due to the partial overlap of the peaks in combination with the deviation of the line shape from a perfect Gaussian, as will be discussed later.

4. Discussion

4.1. Peak width

The peak widths (σ), for H and D in H_2, D_2 and HD, are shown in figure 6. The width was obtained by fitting the peak by a single Gaussian and then subtracting an estimate of the experimental resolution, obtained from Xe measurements under the same conditions. Clearly, the peak width is proportional to the momentum transfer. The proton peak width is always larger than the deuteron peak width. This is understandable, as the Doppler broadening (see equation (1)) is proportional to $1/m_a$. It is also evident that the peak width of H in H_2 is somewhat smaller than the width of H in HD. This is because the zero-point kinetic energy in HD is not equally divided over both atoms. As the centre-of-mass position is not affected by the vibration, the H and D atoms should have opposite momentum. Hence, hydrogen has twice the kinetic energy compared to the D atom. In H_2, the kinetic energy is of course equally divided over both atoms. Thus, in spite of the somewhat lower zero point energy of HD (vibrational energy $\hbar\omega = 0.473$ eV) compared to H_2 ($\hbar\omega = 0.546$ eV), the H kinetic energy, and thus its peak width, is larger in HD than in H_2. Similar considerations hold for D and lead to the conclusion that, in agreement with the experiment, the width of D in D_2 is larger than the width of D in HD.

The peak width is due to the total motion of the atom. It has a vibrational, rotational component as well as a component due to the translational motion of the molecule. Let us first

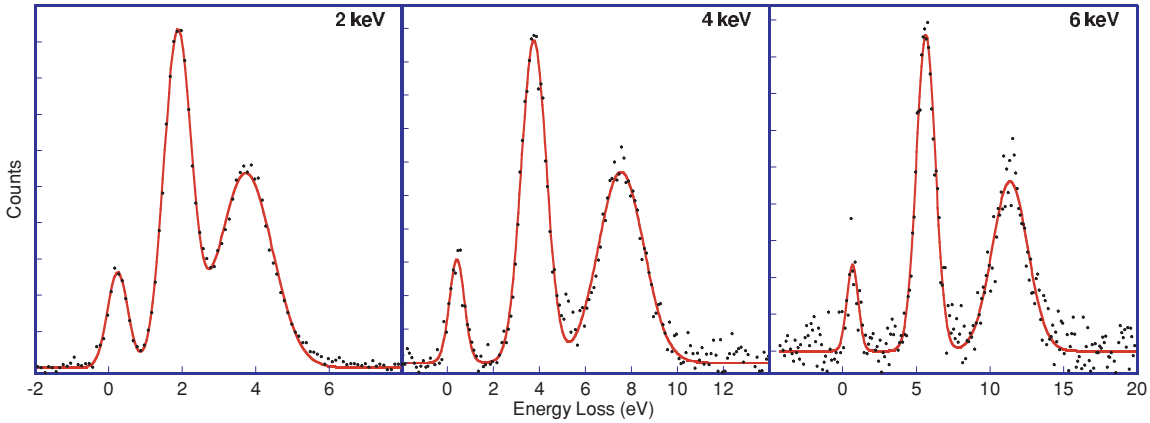

Figure 5. Spectra from HD, at the energies as indicated.

Table 3. A summary of the results for HD.

E_0 (keV)	ΔE calc (eV)	ΔE obs. (eV)	σ D (eV)	σ D corr. (eV)	σ H (eV)	σ H corr. (eV)	I_D:I_H
2.00	1.88	1.85	0.37	0.28	0.72	0.67	1:1.14
4.00	3.76	3.79	0.54	0.46	0.99	0.94	1:1.07
6.00	5.65	5.70	0.64	0.57	1.21	1.17	1:1.01

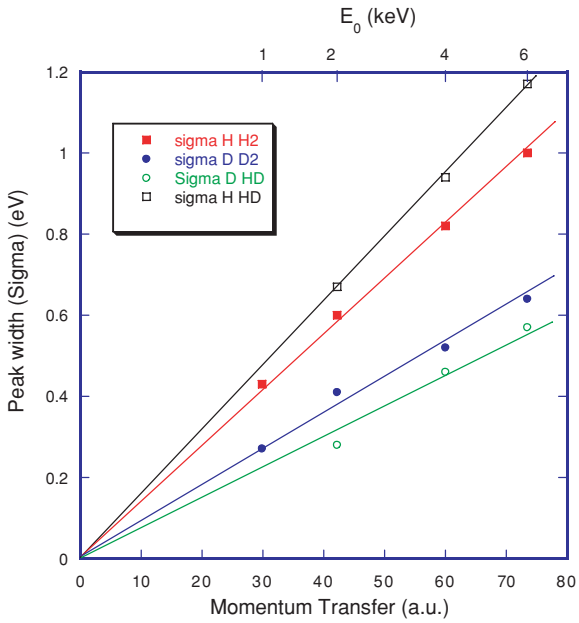

Figure 6. The dependence of the elastic peak width, corrected for energy resolution, on the momentum transfer for H and D in H_2, D_2 and HD.

consider the case of He. Here, the only source of kinetic energy is the translational motion. As was mentioned before, the He peak shape cannot be described by assuming the velocity distribution of a classic gas. This would predict at 6 keV a σ value of 0.37 eV, whereas the raw measured width (0.28 eV) is very close to the experimental resolution (0.25–0.28 eV). Based on this observation, we do not know how to treat the effect of the translational and rotational motions for hydrogen molecules. Based on the vibrational zero point motion alone (resulting in a kinetic energy of $\langle E_{\rm kin}\rangle = 1/8\hbar\omega = 0.068$ eV per atom), one obtains, using equation (2), a value (σ) of 1.01 eV at $E_0 = 6$ keV. This is in good agreement with the observed value (see table 3). Including the two rotational degrees of freedom (energy $2 \times 1/2$ kT, divided over two nuclei) gives an additional kinetic energy of 0.0125 eV per atom, resulting in a width due to rotations and vibrations of 1.1 eV slightly more than the observed width. Finally including the translational energy ($3/2kT$ for the molecule) gives a total energy of $0.068 + 0.0125 + 0.0187 = 0.1$ eV per atom, resulting in a peak width of 1.2 eV, clearly more than the observed width of 1 eV. Thus also for H_2, the target appears much colder than room temperature.

4.2. Peak amplitude

For HD we find, in agreement with Cooper *et al* [13], similar intensities of the H and D peaks. This is in strong contrast to the neutron scattering results of (liquid) HD at the Vesuvio beamline in ISIS, were the H to D peak area ratio was different (by about 30%) from expectations based on well-established cross sections [17]. For a 50% H_2, 50% D_2 mixture, Cooper *et al* found that the H peak area was smaller than the D peak area. Unfortunately we cannot repeat this measurement, as we have no way to verify the effective relative concentration of H_2 and D_2 in the interaction region.

It is instructive, however, to 'simulate' the experiment from Cooper *et al*, using the widths of H and D in the various molecules, as determined in this paper. This is done in figure 7 assuming Gaussian peak shapes. We added the experimental resolution (0.85 eV) of [13] to our resolution-corrected width. In spite of this, our simulated spectra show a slightly better resolution of the H and D peaks. This could be due to the fact that Cooper uses a gas cell, and cooling, due to adiabatic expansion, and/or collimation of the beam will thus

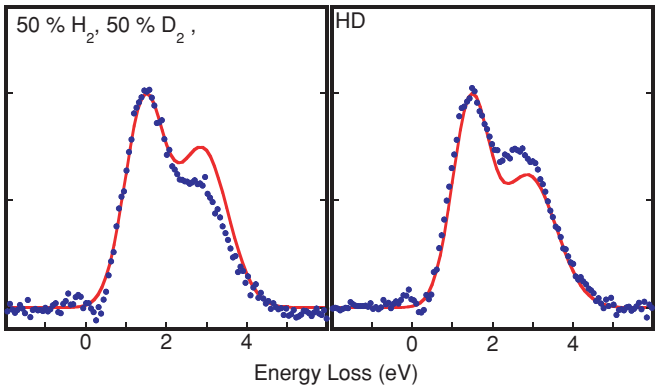

Figure 7. A comparison between the data of [13] (dots) and simulated spectra (lines), based on the intrinsic width as determined in this work.

be absent. Casual inspection of the simulated spectra would suggest that the relative intensity of H in HD is somewhat lower than the H intensity in the 50% H_2, 50% D_2 mixture. This is an illusion caused by the different widths of H and D. However, in the experiment of Cooper the intensity ratio of H appears larger in HD compared to that of the 50% H_2, 50% D_2 mixture. Thus, differences in width do not explain the experimental observation of [13]; in contrast, a fitting procedure based on the width derived in this work would amplify the anomaly.

4.3. Details of the peak shape

So far, we analysed the spectra using a simple Gaussian peak fitting procedure. Either we fit the hydrogen spectra with a single Gaussian or we use the peak shape of a reference gas to determine the spectrometer resolution. The reference gas is usually Xe. Its peak shape deviates from a Gaussian one, and we obtain a much better description of the Xe peak shape if we use the sum of three Gaussians to describe the spectra. The width and position are fitting parameters. We attribute the deviation of the peak shape from simple Gaussian to spectrometer abberations, Maxwell–Boltzmann energy distribution of the incoming beam, etc. Subsequently the hydrogen spectra are described by the same set of Gaussians, but convoluted by an additional Gaussian distribution due to the hydrogen momentum distribution. In the end, a single Gaussian fit and the fit of the broadened sum of three Gaussians give the same quality of description of the hydrogen spectra. The additional broadening due to the momentum distribution completely obscures the deviations of a simple Gaussian response of the spectrometer. This is illustrated in figure 8, together with the background subtraction procedure. However, neither of the procedures gives a fit that describes the spectra within the expected statistical accuracy. There are small, but reproducible, deviations between the experiment and fit. The same tendency is seen in the spectrum for $E_0 = 1$ keV in figure 1 and the spectra below 1 keV in figure 3. Based on neutron scattering work, there are two known reasons why the spectra deviate from a simple Gaussian line shape.

- The failure of the impulse approximation [9, 10]. In the derivation of equation (1) it is assumed that the struck nucleus can be described by a plane wave, as far as the collision is concerned. The nucleus is, however, part of a molecule and has a different set of final states than a free particle. These final state effects are expected to be significant when the recoil energy is not much larger than the energy scale of the internal excitations. For H_2, the vibrational energy (0.546 eV) sets the scale for this effect. Final state effects should become small if the mean recoil energy $\overline{E_r}$ exceeds the vibrational energy by more than a factor of 10. Deviation of a Gaussian line shape, due to final state effects, decreases with increasing E_0. Another signature of final state effects is that they are, in first order, anti-symmetric; in particular, it increases the intensity at $\overline{E_r} + \Delta$ and reduces the intensity at $\overline{E_r} - \Delta$ ($\Delta > 0$) [9].
- The initial momentum distribution of the scattering atom is not described by a single Gaussian. From neutron

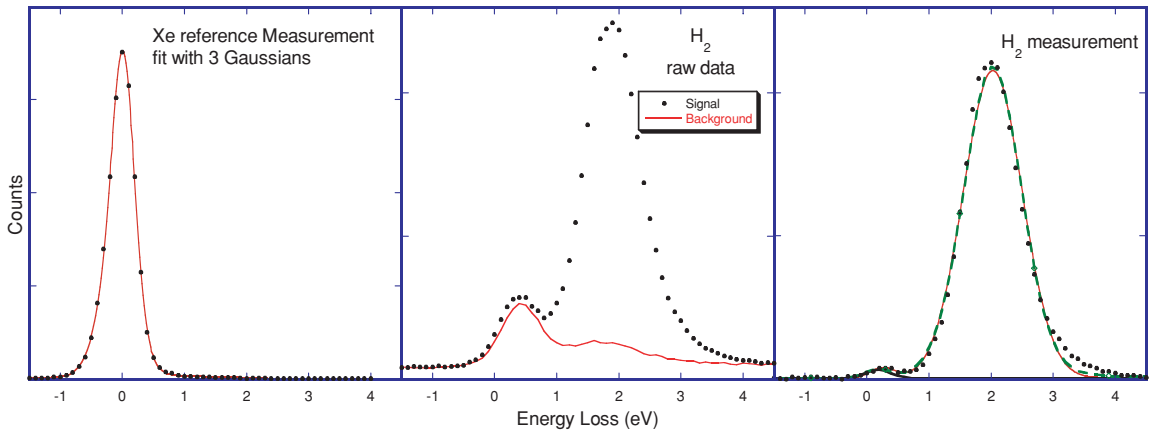

Figure 8. In the left panel, we show an Xe spectrum taken under the same conditions immediately preceding the H_2 measurement. It can be fitted with three Gaussians. This is taken to be the spectrometer resolution function. In the central panel, we show the result of the signal run and background run for H_2. In the difference spectrum, a small fraction of the peak near zero energy loss remains. This is either due to an impurity or due to shortcomings in the background subtraction procedure. This peak can be fitted either with a single Gaussian plus an impurity (full line) or by a resolution function determined from the Xe measurement broadened by a Gaussian + an impurity component (dashed line). Both procedures result in largely equivalent results.

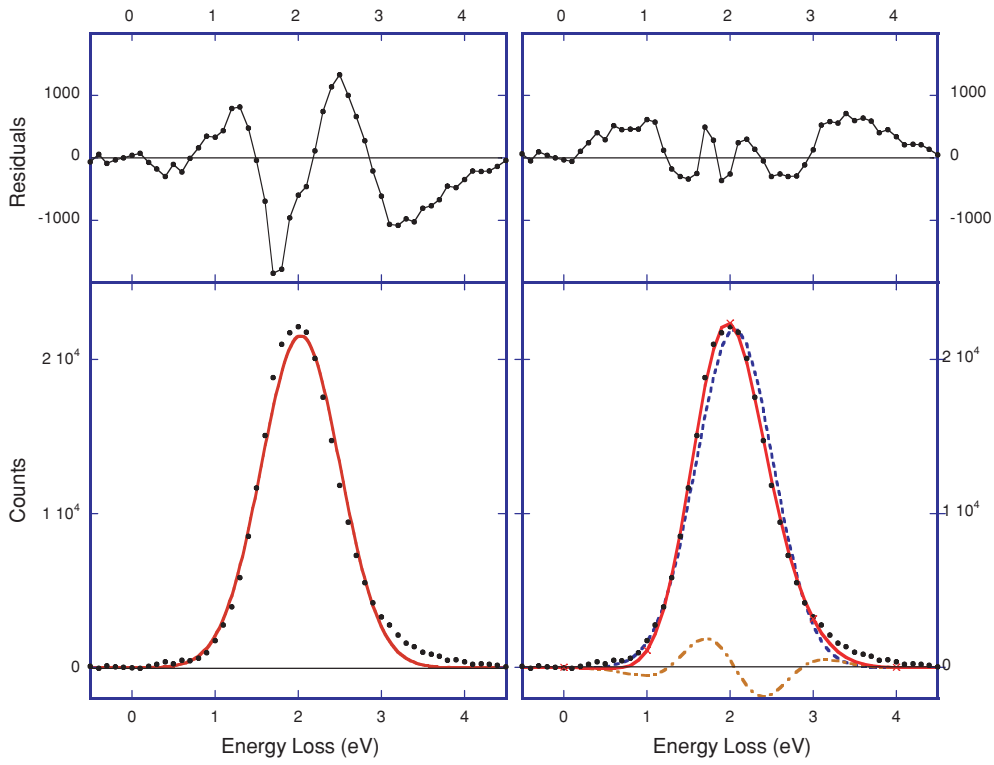

Figure 9. Measurement of a 1 keV electron scattered from H_2 over 135°. In the left panel, the data have been fitted with a single Gaussian. In the right panel, the peak has been fitted with a single Gaussian and the third derivative of this Gaussian. The top panels show the residuals of the fit.

scattering work, we know that at cryogenic temperatures this is indeed the case [8, 11]. Unfortunately, we do not know of any calculations of the hydrogen momentum density at elevated temperatures. Deviations of this type would not cause an asymmetry of the peak. Also, such a deviation would not decrease with increasing momentum transfer.

Thus by studying the energy dependence of the residuals of the Gaussian fit, as well as determining the symmetric/anti-symmetric nature of the residuals, we can judge which of the two mentioned causes dominate. At higher energy it is harder to obtain good statistics, as the cross section decreases as $1/E_0^2$. At low energy the separation of the He and H signal is not complete, and hence the question of symmetric/anti-symmetric nature of the deviation of a Gaussian fit becomes hard to judge as well. Hence, we did a separate run with pure hydrogen. The results of this measurement are shown in figure 9. The data were first fitted using a single Gaussian:

$$I(\epsilon) = c_0\, \mathrm{e}^{-(\overline{E_\mathrm{r}}-\epsilon)^2/2\sigma^2}. \tag{4}$$

As we have no reference gas, there is some uncertainty of the zero of the energy scale and $\overline{E_\mathrm{r}}$ was treated (together with c_0 and σ) as a fitting parameter. Clearly, a single Gaussian does not provide a good description. The residuals appear in first order anti-symmetric with respect to the peak maximum. Adding the leading term of final state corrections, the spectrum would be represented by [9]

$$I(\epsilon) = c_0\, \mathrm{e}^{-(\overline{E_\mathrm{r}}-\epsilon)^2/2\sigma^2} + c_f \frac{\mathrm{d}^3}{\mathrm{d}\epsilon^3}\, \mathrm{e}^{-(\overline{E_\mathrm{r}}-\epsilon)^2/2\sigma^2}. \tag{5}$$

This approach provides a much better fit (with only one additional free parameter: c_f), with reduced residuals that are now mainly symmetric in nature relative to the peak maximum. Whether these residuals are due to deviations of the H Compton profile from Gaussian, or due to higher order final state effects, is beyond the scope of this paper.

5. Conclusion

We studied keV electrons from hydrogen molecules with and without a reference gas. We observed a host of new phenomena, as follows.

- The elastic peak of hydrogen is centred on, or close to, an energy loss value of $q^2/2m_\mathrm{a}$.
- The intrinsic peak width increases proportional to $\sqrt{E_0}$.
- The width of the momentum distribution of the reference gas He along $\widehat{\boldsymbol{q}}$ is much smaller than that of He in equilibrium at room temperature. This can be due to collimation and/or adiabatic expansion.
- Using the well-established vibrational energies of H_2, D_2 and HD, it is clear that the width of the momentum distribution along $\widehat{\boldsymbol{q}}$ of these gases is also smaller than the expected width for these gases in equilibrium.
- The intrinsic peak width of H in HD is larger than that of H in H_2.
- The intrinsic peak width of D in HD is smaller than that of D in D_2.
- Especially for lower values of E_0, it is *not* possible to describe the H peak shape by a Gaussian. Clearly, final

state effects (i.e. failure of the impulse approximation) have an influence on the peak shape. Initial state effects (momentum distribution of H along $\widehat{q}$ is not represented by a Gaussian) could contribute as well.

- These experiments do not corroborate, or are in conflict with, the anomalous scattering cross section reported by Cooper *et al* [13]. In [13] the authors assume that a single width can describe H in H2 and in HD, and another width describing D in both D_2 and HD. Here we show that this assumption is not quite correct, but the deviation is such that using the correct values would enhance the anomaly, rather than reduce it.
- The experiments on HD, especially at higher values of $\overline{E_r}$ where peak decomposition is straightforward, show no sign of a difference in the cross section of H and D. Thus in contrast to neutron scattering from the liquid state [17], there are no anomalies in the present experiment.

Clearly, this survey of electron scattering from hydrogen at high-momentum transfer has revealed a large range of phenomena. Questions remain about the peak shape and the presence of anomalous cross sections. Another important question is what happens at high resolution if $\overline{E_r}$ approaches the vibrational energy of H_2. With better energy resolution, it would be possible to explore the H peak shape for smaller values of q. Final state corrections should become more important as q decreases, and $\overline{E_r}$ becomes comparable to the vibrational energy. Also, the approximation that one scatters from a single H atom (incoherent approximation) would not be valid for low enough q values. As the cross section increases, with decreasing q these experiments are well within reach, even when it requires using a monochromator. In all cases, a comparison with the neutron scattering literature at similar momentum transfer will be very helpful in illuminating the underlying physics. Thus, there are still unexplored topics in the field of electron scattering from hydrogen molecules!

Acknowledgments

The authors want to thank Russel Bonham, Aris Chatzidimitriou-Dreismann, Adam Hitchcock and Erich Weigold for stimulating discussions. This research was made possible by a grant of the Australian Research Council.

References

[1] Vos M 2002 Observing atom motion by electron-atom Compton scattering *Phys. Rev.* A **65** 12703
[2] Vos M and Went M R 2008 Rutherford backscattering using electrons as projectiles: underlying principles and possible applications *Nucl. Instrum. Methods* B **266** 998–1011
[3] Boersch H, Wolter R and Schoenebeck H 1967 Elastische Energieverluste Kristallgestreuter Electronen *Z. Phys.* **199** 124–34
[4] Vos M, Went M R, Cooper G and Chatzidimitriou-Dreismann C A 2008 Elastic electron scattering from methane at high momentum transfer *J. Phys. B: At. Mol. Opt. Phys.* **41** 135204
[5] Herzberg G 1950 *Molecular Spectra and Molecular Structure* (Princeton, NJ: Van Nostrand-Reinhold)
[6] Placzek G 1952 The scattering of neutrons by systems of heavy nuclei *Phys. Rev.* **86** 377–88
[7] Paoli M P and Holt R S 1988 Anisotropy in the atomic momentum distribution of pyrolitic graphite *J. Phys. C: Solid State Phys.* **21** 3633
[8] Mayers J 1993 Measurement of the proton Wave-function in molecular-hydrogen by neutron Compton-scattering *Phys. Rev. Lett.* **71** 1553–6
[9] Sears V F 1984 Scaling and final state interaction in deep inelastic neutron scattering *Phys. Rev.* B **30** 44
[10] Watson G I 1996 Neutron Compton scattering *J. Phys.: Condens. Matter* **8** 5955
[11] Andreani C, Colognesi D, Mayers J, Reiter G F and Senesi R 2005 Measurement of momentum distribution of lightatoms and molecules in condensed matter systems using inelastic neutron scattering *Adv. Phys.* **54** 377–469
[12] Vos M and Went M R 2006 Effects of bonding on the energy distribution of electrons scattered elastically at high momentum transfer *Phys. Rev.* B **74** 205407
[13] Cooper G, Hitchcock A P and Chatzidimitriou-Dreismann C A 2008 Anomalous quasielastic electron scattering from single H_2, D_2, and HD molecules at large momentum transfer: indications of nuclear spin effects *Phys. Rev. Lett.* **100** 043204
[14] Chatzidimitriou-Dreismann C A, Abdul-Redah T, Streffer R M F and Mayers J 1997 Anomalous deep inelastic neutron scattering from liquid H_2O D_2O: evidence of nuclear quantum entanglement *Phys. Rev. Lett.* **79** 2839
[15] Chatzidimitriou-Dreismann C A, Vos M, Kleiner C and Abdul-Redah T 2003 Comparison of electron and neutron Compton scattering from entangled protons in a solid polymer *Phys. Rev. Lett.* **91** 57403
[16] Karlsson E B, Abdul-Redah T, Streffer R M F, Hjörvarsson B, Mayers J and Chatzidimitriou-Dreismann C A 2003 Anomalous neutron Compton scattering cross sections in niobium and palladium hydrides *Phys. Rev.* B **67** 184108
[17] Chatzidimitriou-Dreismann C A, Abdul-Redah T and Krzystyniak M 2005 Anomalous neutron Compton scattering from molecular hydrogen *Phys. Rev.* B **72** 054123
[18] Chatzidimitriou-Dreismann C A, Abdul-Redah T and Sperling J 2000 Sub-femtosecond dynamics and dissociation of C–H bonds in the condensed phase: effects of entangled protonic states *J. Chem. Phys.* **113** 2784–92
[19] Urpelainen S, Huttula M, Kovala P, Makinen A, Calo A, Aksela S and Aksela H 2007 High resolution electron energy loss spectrometer for the study of vapor phase samples *J. Electron Spectrosc. Relat. Phenom.* **156–158** 145–9
[20] Salvat F, Jablonski A and Powell C J 2005 ELSEPA Dirac partial-wave calculation of elastic scattering of electrons and positrons by atoms, positive ions and molecules *Comput. Phys. Commun.* **165** 157–90
[21] Williams J F and Crowe A 1975 The scattering of electrons from inert gases. II. Absolute differential elastic cross sections for neon, krypton and xenon atoms *J. Phys. B: At. Mol. Phys.* **8** 2233–48